Progress In Electromagnetics Research M, Vol. 24, 85–95, 2012

HYBRID FINITE DIFFERENCE/FINITE VOLUME METHOD FOR 3-D CONDUCTING MEDIA PROBLEMS

Z.-L. He*, K. Huang, and C.-H. Liang

Science and Technology on Antenna and Microwave Laboratory, Xidian University, Xi'an 710071, China

Abstract—A hybrid time-domain method combing finite-difference and cell-centered finite-volume method is presented in this paper. This method is applied to solve three dimensional electromagnetic problems which involve media having finite conductivity. The fractional-step technique (FST) for FVTD scheme is applied to solve these problems. Local time-step scheme is used to enhance the efficiency of this method. Numerical results are given and compared with a reliable numerical method, which is used to show the validation of this method.

1. INTRODUCTION

Finite difference time-domain (FDTD) method [1, 2] is a means of directly solving Maxwell's time-dependent curl equations. This method is computationally efficient, but has the limitation that curved surfaces must be approximated using a "stair-cased" representation.

Finite-volume time-domain (FVTD) method has been applied to the numerical solution of Maxwell's equations since 1988 [3–5]. It has benefited from experience gathered previously in finite-volume techniques used in computational fluid dynamics. A great advantage of the FVTD method is its applicability in unstructured meshes. Thus, FVTD method overcomes the problem mentioned before in FDTD method in efficiently simulating structures that include curved or oblique structures.

Based on the location of field components, [6] finite volume formulations can be subdivided into Cell-Centered formulation [7, 8], Cell-Vertex formulation [9] and Cell-Staggered formulation [10]. In Cell-Centered scheme, the degrees of freedom are associated with

Received 25 February 2012, Accepted 2 April 2012, Scheduled 5 April 2012

* Corresponding author: Zhi-Li He (hzl020314@126.com).

barycenters of cells. With the Cell-Centered formulation, a finite volume coincides with the cell itself. Unlike standard FDTD method, the electric and magnetic fields are co-located in space and time within the Cell-Centered FVTD formulation. Cell-Centered scheme is chosen here, because the boundary conditions are taken into account more naturally than the others. In Cell-Vertex formulation, the degrees of freedom are associated with the nodes of cells. The finite volume is defined by connecting the barycenters of cells to which the node belongs. As in FDTD, the field components are staggered in the Cell-Staggered formulas. This formulation can be further classified as E-staggered and H-staggered. In the case of E-staggered formulation, the electric field components are located at the face centers of cells and magnetic field components are at the barycenters of the cells. For H-staggered formulation the location of field components is interchanged.

A hybrid technique FD/FV which builds upon modeling strengths of each algorithm will be a good choice [11, 12]. On the one hand, it is relatively easy to compute FD Cartesian grids. On the other hand, the most essential characteristic of FVTD is its ability to handle unstructured meshes. A numerical scheme based on combining Yee's scheme and a stable Cell-Centered finite volume scheme is introduced. The fractional-step technique FST [7] is applied to treat the conducting media having finite conductivity with complex shape, which will be meshed using unstructured grids and treated by FVTD scheme. Finally, numerical results are given to show that this method is efficient and accurate.

2. GENERAL FORMULATIONS

2.1. Cell-centered FVTD for Conducting Media

The fundamental equations modeling the electromagnetic field in a domain with conducting material are:

$$\begin{cases} \nabla \times \vec{H} - \partial_t \vec{D} - \vec{J} = 0 \\ \nabla \times \vec{E} + \partial_t \vec{B} = 0 \end{cases} . \tag{1}$$

Consider a computation domain V occupied by linear, isotropic, time-invariant, non-dispersive media. Domain V is discretized into elementary volumes $V = \cup_{i=1}^{I} V_i$. Each of these volumes V_i has a boundary surface, ∂V_i, which consists of a number, m_i, of planar facets $\partial V_i = \cup_{k=1}^{m_i} S_{ik}$. The area of S_{ik} will be denoted by s_{ik}.

Integrating (1) over each element V_i and applying the curl theorem, the governing equations can be written as a balance law over the i-th ($i = 1, 2, \ldots, I$) cell V_i, which is assumed to be homogeneous,

as follows:

$$\partial_t \int_{V_i} U\left(\vec{r},t\right) dV = -\alpha_i^{-1} \oint_{\partial V_i} F\left[U\left(\vec{r},t\right)\right] \cdot \vec{n}_i dS_i - \alpha_i^{-1}\kappa_i \int_{V_i} U\left(\vec{r},t\right) dV. \quad (2)$$

where U and $F(U)$ are respectively expressed as:

$$U = \begin{bmatrix} E_x \\ E_y \\ E_z \\ H_x \\ H_y \\ H_z \end{bmatrix}, \quad F(U) = \left[\begin{pmatrix} 0 \\ H_z \\ -H_y \\ 0 \\ -E_z \\ E_y \end{pmatrix}, \begin{pmatrix} -H_z \\ 0 \\ H_x \\ E_z \\ 0 \\ -E_x \end{pmatrix}, \begin{pmatrix} H_y \\ -H_x \\ 0 \\ -E_y \\ E_x \\ 0 \end{pmatrix} \right]. \quad (3)$$

$F\left[U\left(\vec{r},t\right)\right] \cdot \vec{n}_i$ is coined as the "flux" through ∂V_i, and the material matrix can be written as:

$$\alpha_i = \begin{bmatrix} \varepsilon_i \cdot I^{3\times3} & 0^{3\times3} \\ 0^{3\times3} & \mu_i \cdot I^{3\times3} \end{bmatrix}, \quad \kappa_i = \begin{bmatrix} \sigma_i \cdot I^{3\times3} & 0^{3\times3} \\ 0^{3\times3} & 0^{3\times3} \end{bmatrix} \quad (4)$$

where $I_{3\times3}$ is a 3×3 identity matrix, and $0_{3\times3}$ is a 3×3 zero matrix, ε_i, μ_i, and σ_i are the dielectric permittivity, the magnetic permeability, and the electric conductivity of V_i, respectively.

One approach consists in splitting the problem of interest into two subproblems that can be solved independently step-by-step, and to combine their solutions in an alternating manner [13]. The two following subproblems are considered:

$$\partial_t \int_{V_i} U\left(\vec{r},t\right) dV = -\alpha_i^{-1} \oint_{\partial V_i} F\left[U\left(\vec{r},t\right)\right] \cdot \vec{n}_i dS_i. \quad (5)$$

$$\partial_t \int_{V_i} U\left(\vec{r},t\right) dV = -\alpha_i^{-1}\kappa_i \int_{V_i} U\left(\vec{r},t\right) dV. \quad (6)$$

Subproblem (5) is related to the computation of the fields in lossless dielectrics. The Cell-Centered FVTD scheme is based on the computation of both the electric and the magnetic field at the center $\vec{r}_i$ of each element V_i $(i = 1, 2, \ldots, I)$. We denote:

$$u_i^n = U\left(\vec{r} = \vec{r}_i, t = n\Delta t\right) \approx (1/v_i) \cdot \int_{V_i} U\left(\vec{r}, t = n\Delta t\right) dV \quad (7)$$

as the field values at the center of the i-th cell at the n-th temporal time step. As a consequence, the numerical method evaluates u_i^n over N temporal steps of width Δt, being known the initial conditions u_i^0.

Omitting the details of derivation [3], the Cell-Center upwind flux semi-discrete FVTD formulation, applied to the i-th cell takes the form as below:

$$\frac{\partial u_i}{\partial t} = -\frac{\alpha_i^{-1}}{v_i}\left\{\sum_{k=1}^{m_i} s_{ik}\left[\Phi_{ik}^{+}u_{ik}^{-} + \Phi_{ik}^{-}u_{ik}^{+}\right]\right\} \tag{8}$$

where $\Phi_{ik}^{+} = \alpha_i t_{ik} A^{+}\left(\vec{n}_{ik}\right)$, $\Phi_{ik}^{-} = \alpha_j t_{jl} A^{-}\left(\vec{n}_{jl}\right)$, t_{ik} is transmission matrix depending on ε_i, μ_i, α_j and t_{jl} defined just as α_i and t_{ik} but for element V_j which shares a face with cell V_i, S_{ik} or S_{jl}. $A^{+}\left(\vec{n}_{ik}\right)$ and $A^{-}\left(\vec{n}_{jl}\right)$ are furnished in [3] (on page 325). u_{ik}^{+}, u_{ik}^{-} respectively are the values of U inside cell V_j and V_i near the center of S_{ik} (i.e., S_{jl}), which can be interpolated by the cell center field values using the Monotone Upstream-centered Schemes for Conservation Laws (MUSCL) [14].

The second order accurate Lax-Wendroff temporal scheme is adopted. As a consequence, the explicit update equations at the n-th temporal step can be written as:

$$u_i^{n+1/2} = u_i^{n} - \frac{\alpha_i^{-1}\Delta t}{2\cdot v_i}\cdot\sum_{k=1}^{m_i} s_{ik}\left[\Phi_{ik}^{+}u_{ik}^{-,n} + \Phi_{ik}^{-}u_{ik}^{+,n}\right] \tag{9}$$

$$\tilde{u}_i^{n+1} = u_i^{n+1/2} - \frac{\alpha_i^{-1}\Delta t}{v_i}\cdot\sum_{k=1}^{m_i} s_{ik}\left[\Phi_{ik}^{+}u_{ik}^{-,n+1/2} + \Phi_{ik}^{-}u_{ik}^{+,n+1/2}\right] \tag{10}$$

Subproblem (6) is instead on ordinary differential equation taking into account only the effects of conductivity of media, whose solution can be analytically found as follows [7]:

$$\int_{V_i} U\left(\vec{r},t\right)dV = e^{-\alpha_i^{-1}\kappa_i\Delta(t-t_0)}\cdot\int_{V_i} U\left(\vec{r},t_0\right)dV \tag{11}$$

for any t_0, being

$$e^{-\frac{\kappa_i}{\alpha_i}\Delta(t-t_0)} = \mathrm{diag}\left(e^{-\frac{\sigma_i}{\varepsilon_i}\cdot(t-t_0)} \quad e^{-\frac{\sigma_i}{\varepsilon_i}\cdot(t-t_0)} \quad e^{-\frac{\sigma_i}{\varepsilon_i}\cdot(t-t_0)} \quad 1 \quad 1 \quad 1\right) \tag{12}$$

is a 6×6 diagonal matrix. As a consequence, the update of u_i^{n+1} should be modified through the following relation:

$$u_i^{n+1} = e^{-\alpha_i^{-1}\kappa_i\Delta t}\tilde{u}_i^{n+1}. \tag{13}$$

2.2. Hybrid Scheme

Both FDTD and FVTD are local numerical methods: field components at a given point of the grid only depend on its neighbor values. That allows us to locate the hybridization process only at the boundary

between the structured and the unstructured parts of the mesh. By overlapping of one or more cells both on FD/FV meshes, hybrid principle is clear: updating the fields on these cells by using both FDTD and FVTD methods. Partial transition meshes between hexahedral and tetrahedral cells are shown in Fig. 1. There's no difficulty in applying the FVTD scheme for cell A. For cell C, electric and magnetic fields are computed with the FDTD scheme. The field values of cell B should be evaluated by using both FDTD and FVTD methods.

1). If cell B is taken as a cell applied by FVTD scheme, the numerical flux on surface S_{BC} cannot be evaluated because the fields at the center of cell C are not accessible. We do have available the electric fields on the edges of S_{BC} obtained by FDTD scheme. Electric field components can be interpolated to evaluate the required flux:

$$\vec{n}_{S_{BC}} \times \vec{E}^{*}_{S_{BC}} = \vec{n}_{S_{BC}} \times \left(\vec{E}_{y1} + \vec{E}_{y2} + \vec{E}_{x1} + \vec{E}_{x2}\right)\Big/4. \tag{14}$$

According to the continuity of the tangential electric and magnetic field vectors, the magnetic flux can be obtained by:

$$\vec{n}_{S_{BC}} \times \vec{H}^{*}_{S_{BC}} = Y_B \left[\vec{n}_{S_{BC}} \times \vec{n}_{S_{BC}} \times \left(\vec{E}_B - \vec{E}^{*}_{S_{BC}}\right)\right] + \vec{n}_{S_{BC}} \times \vec{H}_B \tag{15}$$

where $\vec{E}_B$, $\vec{H}_B$, Y_B respectively are the electric field, magnetic field and the characteristic admittance of the medium of cell B.

2). When cell B is applied in FD scheme, the electric field along the edges of S_{AB} are averaged by the FV field values in the cells which share the edge with cell B. For instance, $E_x^{S_{AB}}$, can be expressed as:

$$E_x^{S_{AB}} = \left(E_x^A + E_x^B + E_x^{A_1} + E_x^{B_1}\right)/4 \tag{16}$$

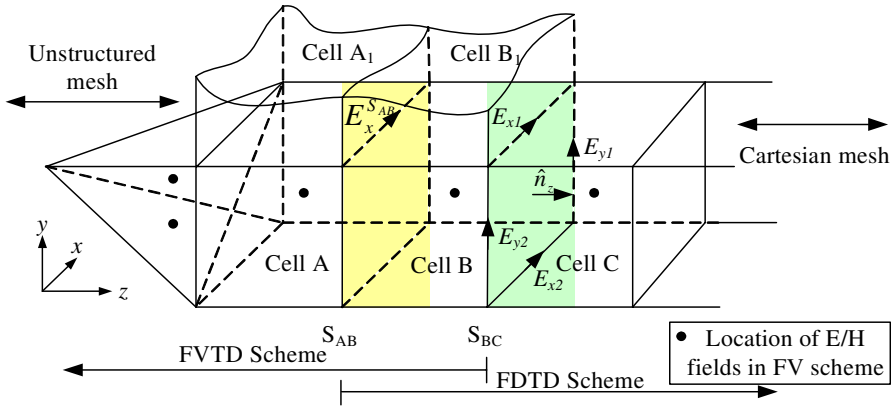

Figure 1. Hybridization mechanism.

where E_x^A, E_x^B, $E_x^{A_1}$, $E_x^{B_1}$ are the electric field values obtained by FVTD scheme. The components along the other three edges of S_{AB} can be calculated just as $E_x^{S_{AB}}$. Thus, component $H_z^{S_{AB}}$ can be updated by using the FDTD scheme with no difficulty.

This method requires nodal coincidence for the two meshes. The interface between the hexahedral and tetrahedral cells is obtained by inserting hexahedral cells where one or several faces are defined by two triangles. This particular cell is treated by using the FVTD method, which offers a correspondence between a quadrilateral face and two triangular faces in terms of the exchange of fluxes. The boundaries of the computational domain, which are located in the structured part of the mesh, are treated by using a PML formalism, as in the purely FDTD approach.

A volume is limited by the surface of the object on one side and a fictitious staircased surface taken in the Cartesian grid at a given distance from the object on the other side (2 cells, for example). This process for obtaining the hybrid mesh is easy to implement and automate. The conducting media structure with curved boundary is located within this volume and is treated by FVTD scheme using FST mentioned above.

3. NUMERICAL RESULTS AND DISCUSSIONS

3.1. Analysis on the Scattering of a Coated Sphere

Firstly, the code is validated by the radar cross section (RCS) prediction for a PEC sphere coated with conducting medium. We

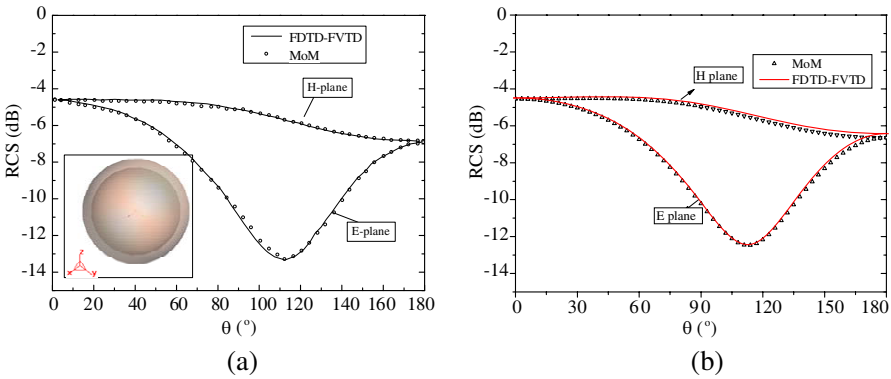

Figure 2. (a) The RCS of the coated sphere; (b) the RCS of the sphere.

consider a perfectly conducting sphere of radius 0.18λ with a dielectric coating 0.02λ. The coating is characterized by a complex, relative permittivity $1.74 - j0.3$. The model is shown in the inset of Fig. 2. The mesh size of the hybrid method is chosen as 0.02λ. A fictitious staircased surface is taken at the distance of 2 cells from the outer sphere, which is set as the boundary of two kinds of meshes. The results obtained by the hybrid method agree very well with that obtained by the method of moment (MOM) [15], as shown in Fig. 2(a). Results without coating are also given in Fig. 2(b). It is shown that the results obtained by the hybrid method agree very well with that obtained by the MOM.

3.2. Analysis on a Rectangular Waveguide with Narrow-wall Slots

In this part, a rectangular waveguide with ten oblique slots in narrow side depicted in Fig. 3 is considered. The waveguide is chosen as the WR-90 waveguide (X-band), with dimensions of $a = 22.86\,\text{mm}$, $b = 10.16\,\text{mm}$, and a wall thickness of $1.27\,\text{mm}$. The material of the wall is assigned as aluminum, whose electric conductivity is $3.8\text{e}+6\,\text{S/m}$. The sizes of slots are designed to set the peak sidelobe level to $-20\,\text{dB}$.

The radiation pattern is calculated by two schemes: pure FDTD method and hybrid FD/FV method. The results are compared with that obtained by a commercially available finite element method (FEM) solver. As shown in Fig. 4, the result obtained by the hybrid method is more accurate than that calculated by the pure FDTD.

For the two schemes mentioned above, the excitation plane is within the region meshed by Cartesian mesh. And the total problem size is: $54 \times 72 \times 448$. For exciting the fundamental TE_{10} mode, we introduce a sinusoid excitation by modifying the updating equation for

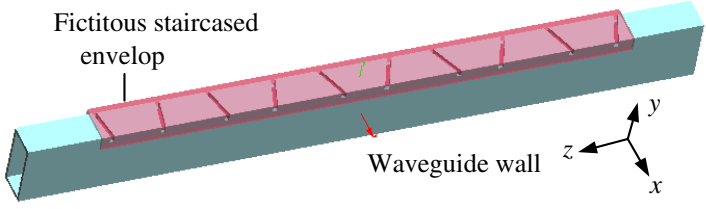

Figure 3. One waveguide with ten oblique slots in narrow side.

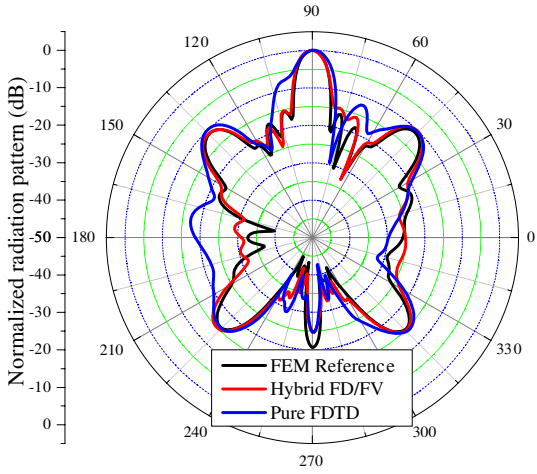

Figure 4. Comparison of the results of the radiation pattern of the H-plane.

the component in the excitation plane as follows:

$$E_y^{n+1}(i,j,k) = g(n\Delta t) + E_y^n(i,j,k) + \frac{\Delta t}{\varepsilon_y(i,j,k)} \cdot \left[\frac{H_x^{n+1/2}(i,j,k+1) - H_x^{n+1/2}(i,j,k)}{\Delta z} - \frac{H_z^{n+1/2}(i+1,j,k) - H_z^{n+1/2}(i,j,k)}{\Delta x} \right] \quad (17)$$

where

$$g(n\Delta t) = \sin(\pi y/a)\sin(2\pi f_0 n\Delta t) \quad (18)$$

in which $f_0 = 9.375\,\text{GHz}$, and the time step Δt satisfying the stability criterion given by:

$$\Delta t \leq 1 \Big/ \left(v\sqrt{(1/\Delta x)^2 + (1/\Delta y)^2 + (1/\Delta z)^2} \right). \quad (19)$$

In this formula, the terms Δx, Δy and Δz denote the spatial step sizes in the directions x, y and z, respectively. Here we set $\Delta x = \Delta y = \Delta z = 0.635\,\text{mm}$. To simulate open boundary structures, it is mandatory to truncate the problem space with appropriate absorbing boundary conditions (ABC). In this paper, UPML scheme is employed to truncate the FDTD grid. At the same time, UPML is applied at the two ends of the waveguide to serve as matched load.

The stability criterion for the FVTD method is:

$$\Delta t \leq \min_{i=1,I} \left[v_i \Big/ \left(v_i \sum_{k=1}^{m_i} s_{ki} \right) \right] \tag{20}$$

where v_i defines the speed of the light in the medium of cell V_i. It is generally more restrictive than that for the FDTD method. A local time step scheme [16] is used to enhance the efficiency of the hybrid method. In addition, it's necessary to constrain the more computationally intensive FVTD to small regions around the objects. The fictitious staircased surface for the hybrid scheme is also shown in Fig. 3. It is taken in the Cartesian grid at a distance of 2 cells to the part of waveguide involve all of the slots. Only the volume bounded by this surface is meshed by unstructured mesh. There are 411507 tetrahedrons in total for this problem. Some unstructured grids shaping the slots are shown in Fig. 5(b), which can more accurate represent the oblique slots than Cartesian mesh shown in Fig. 5(a). For the hybrid method, the minimal time-step of 1.05794 ps for FVTD region and the time step of 4.233 ps for FDTD region were used. Like numerical examples in [16], the hybrid scheme gains in terms of both operations and memory requirements for a solution with a given accuracy in this problem.

The limited accuracy of the FDTD simulation is directly related to the way the corrugation edges are represented. If the edges are approximated using stair-cased — rather than modeled in an appropriate (conformal) way, as shown in Fig. 5(a) — non-physical fields arise from these approximations that do not exist in the actual hardware as designed. In contrast, FVTD inherently uses a conformal mesh and thus non-physical solutions due to meshing do not occur, as shown in Fig. 5(b).

No stability problems have been encountered in our investigations. Nevertheless, theoretical proof of the stability of the hybrid scheme

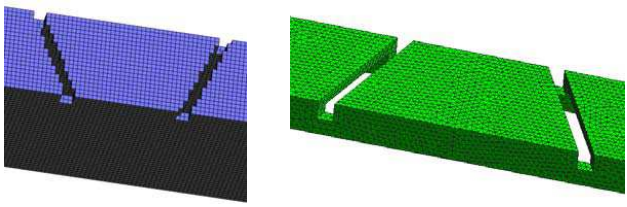

(a) (b)

Figure 5. Partial mesh of narrow-wall slots. (a) Cartesian mesh. (b) Unstructured mesh.

needs to be studied. The hybridization process between the two schemes has been applied on layers penetrate the envelope of the object.

4. CONCLUSION

FST is extended to 3-D case for hybrid FD/FV method in this paper, which preserves the advantages of the finite volume method locally near the geometry of the objects and the simplicity and the speed of the Yee's scheme for areas that are either empty or contain structures with geometries that do not require an unstructured mesh. The method is applied to solve 3-D conducting media problems. Two numerical results are calculated. Compared with the results calculated by reliable methods, the proposed method shows great capability to solve this particular problem precisely. Future work should investigate its application to broad band problems.

ACKNOWLEDGMENT

This work is partly supported by the Fundamental Research Funds for the Central Universities of China (JY10000902002, K50510020017), the National Natural Science Foundation of China (61072019) and the Fund of Science and Technology on Antenna and Microwave Laboratory (9140C070502110C0702).

REFERENCES

1. Yee, K. S., "Numerical solution of initial boundary value problems involving Maxwell's equations in isotropic media," *IEEE Trans. Antennas Propagat.*, Vol. 14, 302–307, May 1966.
2. Taflove, A. and S. C. Hagness, *Computational Electrodynamics: The Finite-difference Time Domain Method*, 2nd edition, Artech House, Norwood, MA, 2000.
3. Bonnet, P., X. Ferrieres, B. L. Michielsen, P. Klotz, and J. L. Roumiguires, *Time Domain Electromagnetics*, Ch. 9, Academic Press, New York, 1999,
4. Shang, J. S., "Characteristic-based algorithms for solving the Maxwell equations in the time domain," *IEEE Antennas Propagat. Mag.*, Vol. 37, 15–25, Jun. 1995.
5. Riley, D. J. and C. D. Turner, "Local tetrahedron modeling of microelectronics using the finite-volume hybrid-grid technique," Sandia Report, SAND95-2790, UC-706, Dec. 1995.

6. Morton, K. W., *Numerical Solution of Convection-diffusion Problems*, Chapman & Hall, London, UK, 1996.
7. Bozza, G., D. D. Caviglia, L. Ghelardoni, and M. Pastorino, "Cell-centered finite-volume time-domain method for conducting media," *IEEE Microwave and Wireless Components Letters*, Vol. 20, No. 9, 477–479, Sep. 2010.
8. Bommaraju, C., "Investigating finite volume time domain methods in computational electromagnetics," Ph.D. Dissertation, Technischen University Darmstadt, Darmstadt, 2009.
9. Andersson, U., "Time-domain methods for the maxwell equations," Ph.D. Dissertation, Department of Numerical Analysis and Computer Science, Royal Institute of Technology, Stockholm, 2001.
10. Remaki, M., "A new finite volume scheme for solving Maxwell's system," *COMPEL*, 913–931, 2000.
11. Yang, M., Y. Chen, and R. Mittra, "Hybrid finite-difference/finite-volume time-domain analysis for microwave integrated circuits with curved PEC surfaces using a nonuniform rectangular grid," *IEEE Trans. Microwave Theory Tech.*, Vol. 48, 969–975, Jun. 2000.
12. Ferrieres, X., J.-P. Parmantier, S. Bertuol, and A. R. Ruddle, "Application of a hybrid finite difference/finite volume method to solve an automotive EMC problem," *IEEE Trans. Electromagnetic Compatibility*, Vol. 46, No. 4, 624–634, Nov. 2004.
13. Leveque, R. J., *Finite Volume Methods for Hyperbolic Problems*, Cambridge University Press, Cambridge, UK, 2004.
14. Haider, F., J.-P. Croisille, and B. Courbet, "Stability analysis of the cell centered finite-volume MUSCL method on unstructured grids," *Numer. Math.*, Vol. 113, 555–600, 2009, DOI 10.1007/s00211-009-0242-6.
15. Medgyesi-Mitschang, L. N., J. M. Putam, and M. B. Gedera, "Generalized method of moments for 3D penetrable scatters," *Opt. Soc. Am. A*, Vol. 11, No. 4, 1383–1398, 1994.
16. He, Z.-L., K. Huang, Y. Zhang, and C.-H. Liang, "A new local time-step scheme for hybrid finite difference/finite volume method," *Journal of Electromagnetic Waves and Applications*, Vol. 26, No. 5–6, 641–652, 2012.